Electrochemical and Solid-State Letters, **10** (1) G1-G4 (2007)
1099-0062/2006/10(1)/G1/4/$20.00 © The Electrochemical Society

Growth Kinetics of Atomic Layer Deposited Hf Silicate-Like Films using $Hf[N(CH_3)(C_2H_5)]_4$ and $SiH[N(CH_3)_2]_3$ Precursors via an H_2O Oxidant

K. B. Chung,[a] M.-H Cho,[b,z] D. W. Moon,[b] D. C. Suh,[c] D.-H. Ko,[c] U. Hwang,[d] and H. J. Kang[d]

[a]*Institute of Physics and Applied Physics and* [c]*Department of Ceramics Engineering, Yonsei University, Seoul 120-749, Korea*
[b]*Division of Advanced Technology, Korea Research Institute of Standards and Science, Daejeon 305-600, Korea*
[d]*Department of Physics, Chungbuk National University, Cheongju, 361-763, Korea*

The growth kinetics of Hf silicate-like films, prepared using $Hf[N(CH_3)(C_2H_5)]_4$ and $SiH[N(CH_3)_2]_3$ precursors and H_2O as an oxidant were investigated as a function of alternating deposition of HfO_2 and SiO_2. The ratio of the alternate deposition of HfO_2 and SiO_2 affected the growth behavior of Hf silicate-like films, but the thickness of the films remained constant, regardless of the total cycles of HfO_2 and SiO_2. The nucleation of HfO_2 showed a strong dependence on the preceding growth cycles of SiO_2, as evidenced by in situ medium energy ion scattering analysis. Hf coverage was reduced with an increasing ratio of SiO_2 deposition cycles. The suppression of the nucleation of HfO_2 is related to remnant Si-H bonds induced by the $SiH[N(CH_3)_2]_3$ precursor after the atomic layer deposited growth of SiO_2.
 [DOI: 10.1149/1.2372222]

Manuscript submitted July 28, 2006; revised manuscript received August 28, 2006. Available electronically November 6, 2006.

The replacement of Si-based oxide with high k dielectric oxides is considered an important step in reducing the electrical oxide thickness required for the scaling of complementary metal oxide semiconductor (CMOS) transistors.[1,2] A higher dielectric oxide makes it possible to reduce excess gate leakage current while increasing the physical thickness. Among the many high k oxides, Hf-silicate is a promising candidate due to its thermal stability when in direct contact with Si at high temperature and its universal channel mobility.[3,4] Although Hf-silicate has a lower permittivity ($\sim$11) than pure HfO_2 ($\sim$25), the incorporation of SiO_2 into HfO_2 can increase the crystallization temperature, thus leading to superior interface properties.

Atomic layer deposition (ALD) has been shown to be an excellent technique for growing conformal thin films with an accurate thickness control and uniformity.[5] A recent study reported that the use of a Hf-amide-type precursor such as $Hf[N(CH_3)(C_2H_5)]_4$ solves problems associated with particles or residual Cl from the halogen based Hf precursor, which is used in ALD Hf-based oxide film growth.[6] Similarly, various Si-amide-type precursors have been used to grow Hf-silicate films. However, it is difficult to obtain SiO_2 rich Hf-silicate films due to the slow deposition rate of SiO_2.[7,8] Among several candidates, $SiH[N(CH_3)_2]_3$ is a good precursor, as it has a very low melting point but a very high vapor pressure. A number of fabrications and characterizations of Hf-silicate films grown using $Hf[N(CH_3)(C_2H_5)]_4$ and $SiH[N(CH_3)_2]_3$ precursors have been carried out.[9,10] On the other hand, very few studies have reported on the growth kinetics of Hf-silicate using ALD due to the reactivity of complex combinations of HfO_2 and SiO_2. In addition, analytic techniques such as in situ measurements for monitoring growth behavior are imprecise. Nevertheless, an understanding of the ALD growth mechanism for Hf-silicate is important for the development of alternatives for SiO_2 because the properties of the dielectric layer depend on controlling the quality of a film and the interface.

In this study, we focused on developing a better understanding of ALD growth kinetics for Hf silicate-like films. We investigated the growth characteristics of Hf silicate-like films as a function of the ratio of alternate deposition cycles between HfO_2 and SiO_2 using liquid precursors of $Hf[N(CH_3)(C_2H_5)]_4$ and $SiH[N(CH_3)_2]_3$ as liquid precursors. The noteworthy findings are that the incorporation of SiO_2 is dominantly related to the change in the nucleation of HfO_2.

Hf silicate-like films were grown on (100) orientated p-type Si wafers that had been cleaned chemically using the standard RCA method to remove organic and metallic residues.[11] After cleaning, the Si wafers were pre-processed to grow an interfacial layer of SiO_2 with a thickness of $\sim$1 nm by means of rapid thermal oxidation (RTO). The Hf silicate-like films were deposited using an ALD system, which has a vertical warm-wall reactor with a shower head and a heated susceptor. The Hf silicate-like films were deposited at a temperature of 280°C using tetrakis(ethylmethylamino)hafnium (TEMAHf), tris(demethlyamono)silane (TDMAS), and H_2O, respectively, as reactant sources for Hf, Si, and O. The feeding time of each of the precursors was 1, 1, 0.2 s, respectively. Each of the sequences were separated by a N_2 purge and a vacuum purge for 100 s to minimize residual gas reactions, such as the chemical vapor deposition (CVD) mode. One cycle of Hf silicate-like films is defined as an alternate deposition ($m + n$), composed of m cycles of HfO_2 and n cycles of SiO_2. To equalize the quantities of supplied Hf during the deposition of Hf silicate-like films, the total number of HfO_2 cycles was fixed at 20 cycles. The reason for fixing the total number of HfO_2 cycles was to make it possible to sensitively measure the difference in growth behaviors of Hf silicate-like films, as medium energy ion scattering (MEIS) that was used as the main measurement results in a high scattering yield in the case of Hf. Growth kinetics were compared by investigating the characteristics of samples deposited with the following cycle combinations: HfO_2 cycle/SiO_2 cycle (Hf/Si) = $1/n$, Hf/Si = $2/n$, Hf/Si = $4/n$, Hf/Si = $5/n$ (n = 1, 3, or 5). The total number of repetitive cycles for the above samples was 20, 10, 5, and 4, respectively.

To obtain elemental and quantitative information in the depth direction, a MEIS analysis was carried out with a 100 keV proton beam in the double-alignment configuration, which reduces contributions from the crystalline Si substrates.[12] The electronic energy loss of 100 keV protons was precisely measured by means of an electrostatic energy analyzer. The incident ions were along the [111] direction, and the scattered ions were along the [001] direction, giving a scattering angle of 125°. A comparison of the relative quantities of hydrogen in the films was performed by elastic recoil detection (ERD) using a 2 MeV He ion. The ERD methods consisted of measuring the energy spectrum of protons that had been elastically hit by incident He ions and recoiled in a forward direction. Fourier transform infrared (FTIR) spectroscopy was used to charac-

[z] E-mail: mhcho@kriss.re.kr

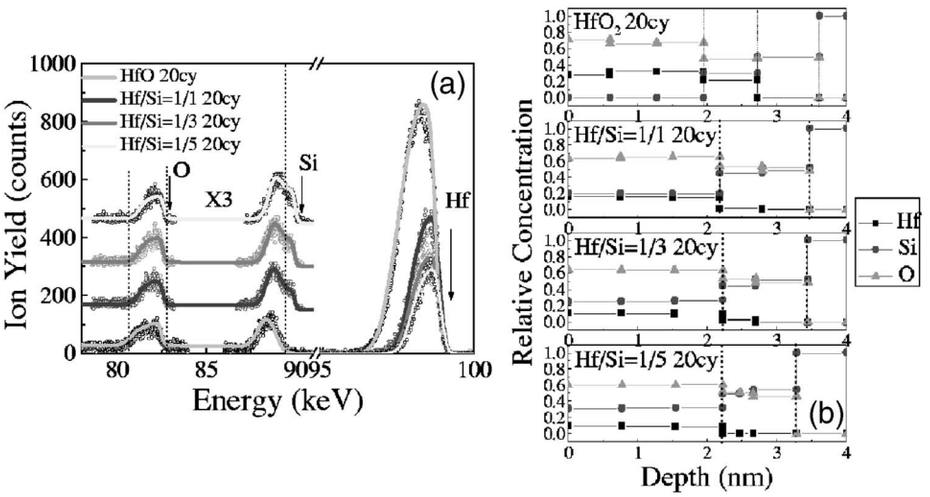

Figure 1. (a) MEIS energy spectra of Hf silicate-like films as a function of the ratio of alternate deposition cycles between HfO_2 and SiO_2 (Hf/Si); Hf/Si = $1/n$ (n = 1, 3, and 5). To equalize the quantities of Hf supplied, the total feeding cycles of Hf were fixed at 20 cycles. (b) Compositional depth profiles corresponding to Fig. 1a.

terize the different bonding arrangements of Hf silicate-like films used in ERD measurement. IR absorption spectra were obtained using the attenuated total reflection (ATR) mode. The ATR mode is most promising, owing to the very high sensitivity realized by internal multiple reflection of the IR light inside an ATR prism. IR absorption spectra were measured with a spectral resolution of 1 cm^{-1}, ranging from 500 to 4000 cm^{-1}.

Figure 1a shows that the backscattering energy spectra of Hf silicate-like films, measured by MEIS, as a function of alternate deposition cycles between HfO_2 and SiO_2 (Hf/Si = m/n). Figure 1 shows the MEIS results of Hf/Si = $1/n$, (n = 1, 3, or 5), respectively. To compare different samples on the basis of HfO_2 initially provided, the total number of HfO_2 cycles was controlled by 20 cycles, while varying the amount of intermediate SiO_2 deposition cycles in different films. In addition, the results on the reference HfO_2 film deposited with 20 cycles without SiO_2 are simultaneously plotted in Fig. 1 to permit the change in Hf coverage depending on the incorporation of SiO_2 to be compared. The most interesting finding is that the Hf coverage decreases, as the ratio of SiO_2 cycles increase. If there were no interactions between HfO_2 and SiO_2, the MEIS results should show the same Hf coverage with the deposition of only 20 cycles of HfO_2 due to the same quantities of Hf fed, regardless of the increase in the ratio of SiO_2 cycles. Another interesting finding is that the O peaks for all samples, indicating the thickness of the deposited oxide films, has the same width, regardless of the total cycles of [(HfO_2 cycles (m) + SiO_2 cycles (n)]. As the total cycles of (HfO_2 cycles + SiO_2 cycles) increase, the thickness of films also generally increase, owing to the linear growth rate of both oxides under the ALD conditions. However, the thickness of all samples was ~2 nm, calculated from the width of O peak, as shown the compositional depth profile in Fig. 1b. Therefore, these results contradicting the ideal behaviors of ALD growth imply that Hf silicate-like films are grown by the interactions between HfO_2 and SiO_2.

For a detailed quantitative analysis, Hf coverage and Si coverage were calculated from simulated results. Figure 2a and b show the changes in Hf coverage and Si coverage depending on the ratio of SiO_2 cycles. Hf coverage decreases with an increase in the ratio of the SiO_2 cycle (n), although an increase in the ratio of the HfO_2 cycle causes an increase in Hf coverage. On the other hand, Si coverage increases with the increase in the ratio of SiO_2 cycle (n). In addition, the Si coverage tend to increase with total SiO_2 cycles. These results indicate that Hf coverage is affected by the ratio of SiO_2 deposition cycles, and are confirmed by the fact that Hf coverage including SiO_2 is lower than that of HfO_2 (20 cycles) without the incorporation of SiO_2, represented in the energy spectra of Fig. 1a. In other words, the SiO_2 growth cycles that precede the HfO_2 deposition suppress the nucleation of HfO_2.

To confirm the effect of the incorporation of SiO_2 on the nucleation of HfO_2, the growth of HfO_2 on HfO_2 (4 cycles) + SiO_2 (5 cycles) was compared with the growth of HfO_2 on only HfO_2 (4 cycles) by in situ MEIS monitoring. The initial 4 cycles of HfO_2 result in a HfO_2 coverage over ~1 mL. These 5 cycles of SiO_2 could be regarded as an amount sufficient to cover the preceding HfO_2 layer with SiO_2. The increase in the area of the Hf peak on 4 cycles of HfO_2 is higher, as shown in energy spectra of Fig. 3a. The calculated Hf coverage on HfO_2 (4 cycles) + SiO_2 (5 cycles) is entirely lower than that on HfO_2 (4 cycles), as shown in Fig. 3b. The drastic difference in Hf coverage is especially evident for the first additional cycle of HfO_2. The subsequent nucleation of HfO_2 is affected by differences in surface conditions, according to the presence of SiO_2 layer.

The ALD growth of HfO_2 is generally affected by the OH density on the surface and is prevented by the others except OH bonds, such as H bonds.[13-15] Therefore, H bonding related to the ALD surface reactions could have an effect on the nucleation of the following metal precursors. ERD was used to determine the total hydrogen content in the films. Figure 4a shows the ERD spectra as a function of the ratio of SiO_2 cycles (n = 1, 3, or 5), for the ratio of HfO_2 cycles is 1 cycle and the total number of HfO_2 cycles is 20. ERD spectra of only HfO_2 (20 cycles) were simultaneously measured to compare with the change in hydrogen content in the films as the result of the incorporation of SiO_2. As the ratio of SiO_2 cycle increases, the area of the ERD spectra is increased. The quantities of

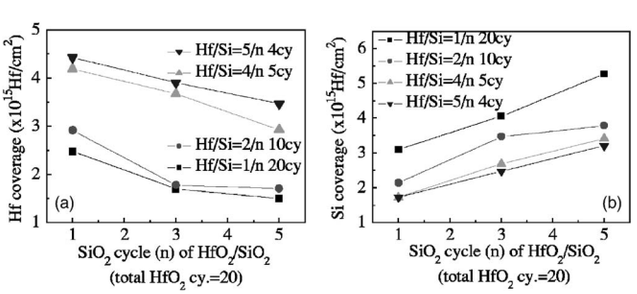

Figure 2. (a) Calculated Hf coverage depending on the ratio of SiO_2 cycle. (b) Calculated Si coverage depending on the ratio of SiO_2 cycle.

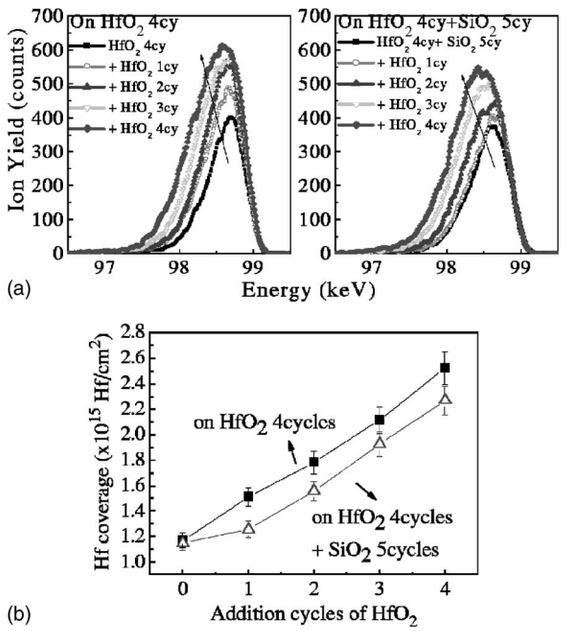

Figure 3. (a) The in situ MEIS energy spectra in the Hf region depending on the initial surface conditions as a function of additional HfO_2 cycles (4 cycles of HfO_2 and 4 cycles of HfO_2 + 5 cycles of SiO_2). (b) The comparison of the calculated Hf coverage depending on the initial surface conditions as a function of additional HfO_2 cycles (4 cycles of HfO_2 and 4 cycles of HfO_2 + 5 cycles of SiO_2).

hydrogen contents from ERD data show the following order; HfO_2 20cy < Hf/Si = 1/1 < Hf/Si = 1/3 < Hf/Si = 1/5. This implies that the total hydrogen content is increased along with an increase in the ratio of SiO_2 cycles. The inset of Fig. 4a shows the calculated relative area for the ERD spectra, excluding the hydrogen content of HfO_2 (20 cycles). The tendency for the hydrogen content to be related to the increase in the ratio of SiO_2 cycles increases linearly. Although the total hydrogen content increases with an increase in the ratio of SiO_2 cycle, the quantities of hydrogen measured by ERD represent the total amounts of bonded and nonbonded hydrogen in the films. In other words, hydrogen measured by ERD could result from contamination or remnant H bonds. Consequently, it is necessary to determine the bonding characteristics of hydrogen content that remains.

Figure 4b shows IR absorption spectra of Hf/Si = 1/3 and Hf/Si = 1/5, in which the total number of HfO_2 cycles was fixed at 20 cycles. For a comparison and reference of the Si-H stretching vibration, HfO_2 (20 cycles) and H-terminated Si were measured. The Si-H stretching vibration modes from IR absorption spectra show the following tendencies; HfO_2 20cy < Hf/Si = 1/3 < Hf/Si = 1/5 < H-terminated Si. The H-terminated surface exhibits two representative peaks for Si-H bonds at ~2080 and ~2110 cm^{-1}, corresponding to monohydride Si (SiH) and dihydride Si (SiH_2), respectively.[16-18] The Si-H stretching vibration spectrum for the H-terminated Si(100) surface is characterized by an intense SiH_2 peak. This is simply due to the fact that the ideal, bare Si(100) surface has two dangling bonds per Si atom, and the hydrogen termination of those dangling bonds produces dihydride Si. In the case of HfO_2, the intensity of the hydride modes, SiH and SiH_2, decreases after film growth in comparison with H-terminated Si. This is due to thermal oxidation prior to the film growth. However, Hf silicate-like films shows higher Si-H stretching vibration modes, indicating that the Si-H bonds in Hf silicate-like films are higher than that in HfO_2. In addition, as the ratio of SiO_2 cycle increases, the Si-H stretching vibration modes increase slightly. These results are consistent with the hydrogen content in the previous ERD data. Therefore, the increase in Si-H bonds with an increase in the ratio of SiO_2 cycles indicates that the ALD reaction using $SiH[N(CH_3)_2]_3$ could allow the Si-H bonds to remain in the films, because the growth of SiO_2 by thermal oxidation causes a decrease in the total number of Si-H bonds.[19]

$SiH[N(CH_3)_2]_3$ is composed of one Si-H bond and three Si-$N(CH_3)_2$ bonds. These two bonds have different bond strength, which have been calculated using various theoretical approaches, such as ab initio calculations and density-functional calculations.[20,21] The energy of the Si-H bond is 2.9–3.7 eV, whereas the energy of Si-$N(CH_3)_2$ bond is ~2.7 eV. This means that the Si-H bond is stronger than Si-$N(CH_3)_2$ bond. For the remaining probability after the ALD process, the Si-H bond is higher than Si-$N(CH_3)_2$ bond due to the difference in bond strength. These different bond strengths between Si-H and $SiN(CH_3)_2$ bonds leads to a discrepancy in the exchange reaction rates during the feeding the Hf or Si precursors. Therefore, the nucleation of HfO_2 on the preceding growth of SiO_2 would be prevented due to the remnant Si-H bonds after the growth of SiO_2.

In summary, the growth kinetics of Hf silicate-like films, prepared using $Hf[N(CH_3)(C_2H_5)]_4$ and $SiH[N(CH_3)_2]_3$ precursors via H_2O as an oxidant were investigated as a function of the alternate deposition of HfO_2 and SiO_2. The nucleation of HfO_2 shows a strong dependence on the preceding growth of SiO_2. Hf coverage is reduced with an increase in the ratio of SiO_2 deposition cycles. The surface condition of the remnant Si-H bonds induced by $SiH[N(CH_3)_2]_3$ precursor after ALD growth of SiO_2 inhibits the subsequent nucleation of the Hf precursor.

This work was partially supported by the National Program for Tera-level Nanodevices of the Ministry of Science and Technology as one of the 21 Century Frontier Programs.

The Korea Research Institute of Standards and Science assisted in meeting the publication costs of this article.

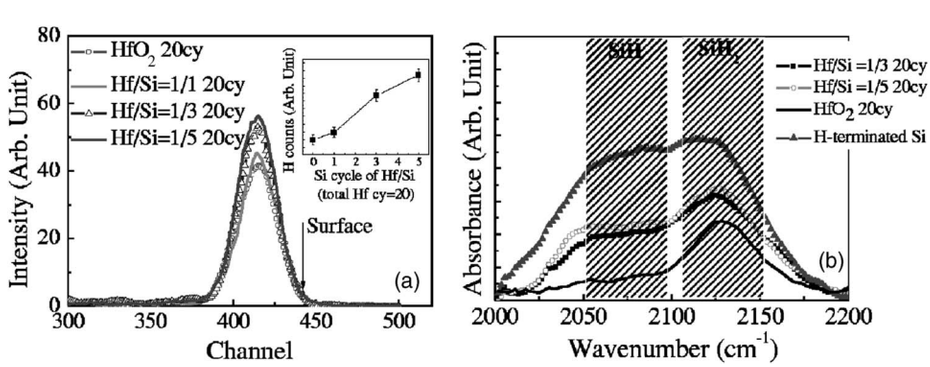

Figure 4. (a) ERD spectra of HfO_2, and Hf silicate films as a function of the ratio of SiO_2 cycles (n = 1, 3, or 5), with a total cycles of HfO_2 of 20. The inset is the calculated relative area of the ERD spectrum, excluding the hydrogen content of HfO_2 (20 cycles). (b) IR absorption spectra of Hf/Si = 1/3 and Hf/Si = 1/5. For a comparison and reference of Si-H stretching vibration, the results of HfO_2 and H-terminated Si are plotted simultaneously.

References

1. G. D. Wilk, R. M. Wallace, and J. M. Anthony, *J. Appl. Phys.*, **89**, 5243 (2001).
2. A. I. Kingon, J.-P. Maria, and S. K. Streiffer, *Nature (London)*, **406**, 1032 (2000).
3. G. D. Wilk, R. M. Wallace, and J. M. Anthony, *J. Appl. Phys.*, **89**, 5243 (2001).
4. H. Watanabe, M. Saitoh, N. Ikarashi, and T. Tatsumi, *Appl. Phys. Lett.*, **85**, 449 (2004).
5. R. L. Puurunen, *J. Appl. Phys.*, **97**, 121301 (2005).
6. X. Liu, S. Ramanthan, A. Longdergan, A. Srivastava, E. Lee, T. E. Seidel, J. T. Barton, D. Pang, and R. G. Gordon, *J. Electrochem. Soc.*, **152**, G213 (2005).
7. S. Kamiyama, T. Miura, and Y. Nara, *Electrochem. Solid-State Lett.*, **8**, F37 (2005).
8. S.-W. Kang, S. W. Rhee, and S. M. George, *J. Vac. Sci. Technol. A*, **22**, 2392 (2004).
9. K. B. Chung, C. N. Whang, M.-H. Cho, C. J. Yim, D.-H. Ko, Y.-S. Kim, M. J. Kim, J. -H Lee, and N. I. Lee, *J. Korean Phys. Soc.*, **48**, 607 (2006).
10. S. Kamiyama, T. Miura, Y. Nara, and T. Arikado, *Electrochem. Solid-State Lett.*, **8**, G215 (2005).
11. W. Keren, *RCA Rev.*, **31**, 207 (1970).
12. J. F. van der Veen, *Surf. Sci. Rep.*, **5**, 199 (1985).
13. T. Suntola, *Appl. Surf. Sci.*, **100/101**, 391 (1996).
14. M. L. Green, M.-Y. Ho, B. Busch, G. D. Wilk, T. Sorsch, T. Conard, B. Brijs, W. Vandervorst, P. I. Raisanen, D. Muller, M. Bude, and J. Grazul, *J. Appl. Phys.*, **92**, 7168 (2002).
15. K. B. Chung, C. N. Whang, H. S. Chang, D. W. Moon, and M.-H. Cho, In preparation.
16. T. Miura, M. Niwano, D. Shoji, and N. Miyamoto, *J. Appl. Phys.*, **79**, 4373 (1996).
17. Y. J. Chabal, G. S. Higashi, K. Raghavachari, and V. A. Burrows, *J. Vac. Sci. Technol. A*, **7**, 2104 (1989).
18. M. Niwano, M. Terashi, and J. Kuge, *Surf. Sci.*, **420**, 6 (1999).
19. T. Miura, M. Niwano, D. Shoji, and N. Miyamoto, *J. Appl. Phys.*, **79**, 4373 (1996).
20. M. B. Raschke and U. Hofer, *Phys. Rev. B*, **63**, 201303 (2001).
21. J.-H. Cho and L. Kleinman, *Phys. Rev. B*, **68**, 245314 (2003).